

# Supporting Information for “The Role of Clouds in Shaping Tropical Pacific Response Pattern to Extratropical Thermal Forcing”

Wei-Ting Hsiao<sup>1,2</sup>, Yen-Ting Hwang<sup>1</sup>, Yong-Jih Chen<sup>1</sup>, and Sarah M. Kang<sup>3</sup>

<sup>1</sup>Department of Atmospheric Sciences, National Taiwan University, Taipei, Taiwan

<sup>2</sup>Department of Atmospheric Science, Colorado State University, Fort Collins, CO, USA

<sup>3</sup>School of Urban and Environmental Engineering, Ulsan National Institute of Science and Technology, Ulsan, South Korea

## Contents of this file

1. Text S1 to S2
2. Figure S1
3. Table S1

**Introduction** The supporting information includes (1) a section of text describing experimental settings in detail, (2) a supplementary figure that is mentioned but not present in the main text, and (3) a table that describe all the simulations that were conducted.

---

## Text S1. Model setting

### S1.1 Experimental Design

Community Earth System Model 1.2 (CESM 1.2; Hurrell et al., 2013) has been employed to perform the experiments in this study. The atmospheric model, Community Atmosphere Model 5.0 (CAM5; Neale et al., 2010), is used with an active seasonal cycle and spatial resolution of  $1.9^\circ$  latitude by  $2.5^\circ$  longitude and 30 vertical layers. Realistic continental distribution and topography is used. Vegetation, aerosols, and greenhouse gases are set to pre-industrial conditions. The oceanic model, Parallel Ocean Program 2.0 (POP2), is used with the grid system of gx1v6, which is approximately  $1^\circ$  by  $1^\circ$  horizontally.

In the slab-ocean setting, the default POP2 grid in vertical direction is replaced by a single-layer slab ocean of a homogeneous depth of 50 meters. A  $q$  flux with seasonal cycle obtained by the time-mean data of the control run in a fully coupled setting, which represents the convergence of climatological oceanic heat transport, are prescribed in the slab ocean. Dynamical oceanic interactions with other components of the model are absent in this setting. A control simulation (CTL) using the historical scenario of the 1850s is performed. Two perturbed simulations are branched from a same arbitrary year of CTL, in which the surface heating is imposed into the slab ocean as additional  $q$  flux over either the Northern Atlantic (hNA) and the Northern Pacific (hNP). The heating is roughly imposed between  $45^\circ\text{N}$  and  $65^\circ\text{N}$  zonally uniformly with a meridional half-sine shape. The peak values of the heating are about  $69.5 \text{ W m}^{-2}$ , and the total amount of each heating field is adjusted to be approximately 0.41 petawatts by modifying the latitudinal range

slightly. Note that the area of heating avoids where the annual maximum sea ice cover is over 0.5 to prevent severe effects from direct melting of ice. For the time length that each simulation has been run out to, see Table S1. The perturbed simulations have reached equilibria with the time ran as their global mean imbalances of top-of-the-atmosphere (TOA) flux lie within positive and negative  $0.15 \text{ W m}^{-2}$ , which is similar to the value from CTL ( $0.13 \text{ W m}^{-2}$ ). To reproduce the simulations, use the *compset* E1850C5.

To investigate cloud radiative effects, we use a cloud-locking (CL) method in CAM5 (Ceppi & Hartmann, 2016; Chen et al., 2021) with the slab-ocean setting to verify the role of clouds. Hourly cloud optical properties of the control run are prescribed in the simulations of cloud locking. A control simulation (CTL-CL) is performed, which is branched from an arbitrary year in CTL and cloud radiative properties from CTL are then being imposed from another arbitrary year in CTL to capture the decoupling effect between cloud radiative properties and other fields. Two perturbed simulations (hNA-CL and hNP-CL) are branched from a same arbitrary year in CTL, when the idealized surface heating and the CTL cloud optical properties are started to be imposed. Similarly, the perturbed simulations have reached equilibria that their global mean imbalances of TOA flux lie within  $0.11 \text{ W m}^{-2}$ , which are similar to the value from CTL-CL ( $0.11 \text{ W m}^{-2}$ ). We could then obtain the responses to heating without cloud effect by subtracting any fields from CTL-CL from either hNA-CL or hNP-CL. Finally, the cloud effect is obtained by subtracting the responses to heating with cloud effect by those without cloud effect.

We also conduct a set of fully coupled (FOM) experiments with two idealized forcing to investigate the importance of the processes discussed in the slab-ocean experiments with

oceanic dynamical responses. The ocean model is set to be dynamically interactive with 60 vertical layers and with realistic oceanic topography. A control simulation (CTL-FOM) is performed. In the perturbed simulations (hNA-FOM and hNP-FOM), the idealized surface heating is imposed in the form of additional downward longwave radiative flux with the horizontal spatial structures same as in the slab-ocean heating simulations. To show the transient responses to the extratropical forcing, multiple ensembles of FOM heating experiments are performed (see Table S1 for detail). To reproduce the simulations, use the *compset* B1850C5.

### **S1.2 Technical details of implementing cloud locking**

In the radiation scheme of CAM5 (RRTMG; Iacono et al., 2008), a number of cloud properties are used in the calculation of radiative fluxes (Pincus et al., 2003). Those variables include cloud fraction, snow cloud fraction, in-cloud liquid/ice/snow water path, effective diameter for ice and snow, and size distribution parameters. From the control simulations (CTL-SOM and CTL-FOM), we save the instantaneous fields of these variables whenever the radiation module is called (i.e., every hour). Next, in the cloud-locking simulations, we prescribe the cloud properties in the radiation calculation with the cloud fields saved beforehand. This is done by overwriting the cloud properties in the following subroutines:

1. radiation\_tend
2. get\_liquid\_optics\_sw
3. get\_ice\_optics\_sw
4. get\_snow\_optics\_sw

- 5. snow\_cloud\_get\_rad\_props\_lw
- 6. ice\_cloud\_get\_rad\_props\_lw
- 7. liquid\_cloud\_get\_rad\_props\_lw

By doing so, the radiation module would always use the prescribed cloud properties in the calculation of radiative fluxes, instead of the cloud properties in the current simulation.

## **Text S2. The derivation of the attribution of SST anomalies to surface and oceanic mixed-layer energy fluxes**

An energy budget analysis of oceanic mixed layer is used to attribute SST response to each surface energy flux (Xie et al., 2010; Zhang & Li, 2014). First, we assume that the temperature is uniform across the mixed layer including its surface. The time tendency of the mixed-layer temperature ( $T$ ) can be written as:

$$T_t = \frac{1}{\rho c_p H} (Q_{SW} + Q_{LW} + Q_{LH} + Q_{SH} + Q_{C_o})$$

where subscript  $t$  denotes time derivative, the density of sea water,  $c_p$  the specific heat capacity at constant pressure of sea water,  $H$  the mixed-layer depth, and  $Q$  the inward energy flux. Fluxes include shortwave (SW) and longwave (LW) radiative fluxes, latent heat flux (LH), sensible heat flux (SH), and column-integrated heat convergence by the transport of ocean currents ( $C_o$ ), with the sign convention that positive heats the surface. Since  $Q_{C_o}$  is not directly provided by the model, it is calculated by the following formula:

$$Q_{C_o} = - \int_{-H}^{surface} \nabla \cdot (\vec{V} H_{OHC}) dz$$

where  $H$  denotes mixed-layer depth,  $\vec{V}$  is oceanic current, and  $H_{OHC}$  is the oceanic heat content. Here, the mean H of the forced states and the control state are used, so the effect

of the change in mixed layer thickness is omitted during the calculation. Another step to note is that the model output  $H$  is continuous while the ocean vertical grid points are discrete and scarce compared to the change in  $H$ , thus the vertical integral is calculated assuming that the vertical variations of  $\vec{V}$  and  $H_{OHC}$  are linear between the grid points.

In SOM experiments,  $Q_{C_o}$  is unchanged by design (represented as  $q$  flux) and the system reaches equilibrium thus the total  $T_t = 0$ . The temperature difference between the control state and the forced state could be written as:

$$\Delta T_{flux} = \frac{1}{\overline{dQ/dT}} \Delta Q_{flux}, \quad flux = \{SW, LW_{dn}, LH_a, SH\}$$

where  $\Delta$  denotes the differences between the forced state and the control state,  $\overline{dQ/dT}$  is the linear dependence of total surface energy flux to  $T$  evaluated at the mean states between the forced and the control states, which consists of a blackbody longwave radiative term ( $4\sigma T^3$ ) and a latent heat term associated with its bulk formula ( $L_v Q_{LH}/RT^2$ ). Note that sensible heat flux also has a linear dependency on the surface temperature, but is omitted because its high nonlinearity leads to unreasonable magnitudes of values when implementing our calculation procedure. After removing the linear dependent terms to  $T$ , downward longwave radiative flux ( $LW_{dn}$ ) and non-Newtonian latent heat flux that depends solely on near-surface atmospheric condition ( $LH_a$ ) appear that replace LW and LH, respectively. The complete expression of  $\Delta T_{flux}$  is:

$$\Delta T_{flux} = \frac{1}{4\sigma \bar{T}^3 + L_v \overline{Q_{LH}} / R \bar{T}^2} \Delta Q_{flux}, \quad flux = \{SW, LW_{dn}, LH_a, SH\}$$

where the overbar denotes the mean states of the forced and the control states (simply calculated as the arithmetic means of the two states) as this method is essentially utilizing a Taylor's expansion with respect to a certain state. Finally, we note that all the calcu-

lations are done for each calendar month and annual means are calculated as the final step.

## References

- Ceppi, P., & Hartmann, D. L. (2016, January). Clouds and the atmospheric circulation response to warming. *J. Clim.*, *29*(2), 783–799.
- Chen, Y.-J., Hwang, Y.-T., & Ceppi, P. (2021, October). The impacts of Cloud-Radiative changes on poleward atmospheric and oceanic energy transport in a warmer climate. *J. Clim.*, *34*(19), 7857–7874.
- Hurrell, J. W., Holland, M. M., Gent, P. R., Ghan, S., Kay, J. E., Kushner, P. J., ... Marshall, S. (2013, September). The community earth system model: A framework for collaborative research. *Bull. Am. Meteorol. Soc.*, *94*(9), 1339–1360.
- Iacono, M. J., Delamere, J. S., Mlawer, E. J., Shephard, M. W., Clough, S. A., & Collins, W. D. (2008, July). Radiative forcing by long-lived greenhouse gases: Calculations with the AER radiative transfer models. *J. Geophys. Res.*, *113*(D13).
- Neale, R. B., Chen, C.-C., Gettelman, A., Lauritzen, P. H., Park, S., Williamson, D. L., ... Others (2010). Description of the NCAR community atmosphere model (CAM 5.0). *NCAR Tech. Note NCAR/TN-486+ STR*, *1*(1), 1–12.
- Pincus, R., Barker, H. W., & Morcrette, J.-J. (2003, July). A fast, flexible, approximate technique for computing radiative transfer in inhomogeneous cloud fields. *J. Geophys.*

*Res.*, 108(D13).

Xie, S.-P., Deser, C., Vecchi, G. A., Ma, J., Teng, H., & Wittenberg, A. T. (2010, February). Global warming pattern formation: Sea surface temperature and rainfall.

*J. Clim.*, 23(4), 966–986.

Zhang, L., & Li, T. (2014, November). A simple analytical model for understanding the formation of sea surface temperature patterns under global warming. *J. Clim.*,

27(22), 8413–8421.

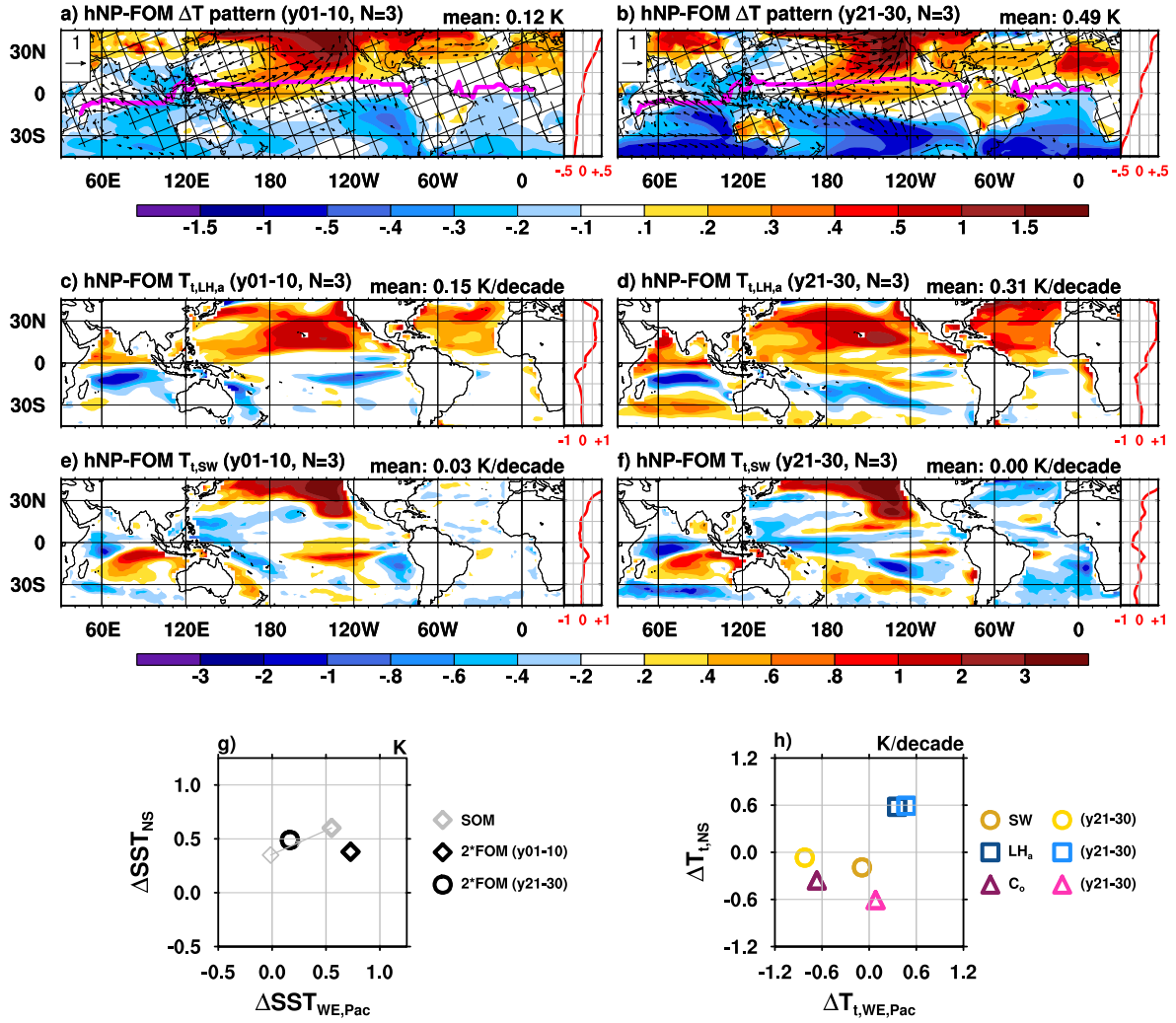


**Figure S1.** Results from the fully coupled North Pacific heating experiments (hNP-FOM): (a-b) as Figures 4a-b; color shadings in (c-d) are as Figures 2d and (e-f) are as Figures 2f, but of the associated SST tendencies (K decade<sup>-1</sup>) over the two time periods; (g-h) as Figures 4e-f. Note that the SST gradient metrics are not perfectly suitable for presenting the results from hNP-FOM runs: for example, in (h) the SST tendency contributed by SW does not enhance the  $\Delta T_{t,WE,Pac}$  over the first ten years, however, a clear spatial pattern of  $T_{t,SW}$  that follows the climatological cloud regime is shown in (e) that enhances the zonal SST gradient locally over the central and the eastern tropical Pacific. We argue that the mechanisms of the SST pattern formation that highlight the importance of clouds proposed in the main text are still important here, but are manifested differently with a more complicated spatial distribution of SST-cloud feedbacks.

**Table S1.** The experiment list

Name	Descriptions	Simulated	Years	Ensemble
		Years	Analyzed	Counts
CTL-SOM	Preindustrial control simulation with a slab-ocean lower boundary	95	70	1
hNA-SOM	Surface thermal heating added in the extratropical North Atlantic with a slab-ocean lower boundary	65	30	1
hNP-SOM	As hNA-SOM but with extratropical North Pacific heating	65	30	1
CTL-SOM-CL	As CTL-SOM but cloud properties are locked to those in different years from CTL-SOM	40	30	1
hNA-SOM-CL	As hNA-SOM but cloud properties are locked to those from CTL-SOM	40	20	1
hNP-SOM-CL	As hNP-SOM but cloud properties are locked to those from CTL-SOM	40	20	1
CTL-FOM	Preindustrial control simulation with a dynamical-ocean lower boundary	120	120	1
hNA-FOM	Surface thermal heating added in the extratropical North Atlantic with a dynamical-ocean lower boundary	30	1-10 21-30	8 (year 1-10) 3 (year 21-30)
hNP-FOM	As hNA-FOM but with extratropical North Pacific heating	30	1-10 21-30	3 (year 1-10) 3 (year 21-30)
CTL-FOM-CL	As CTL-FOM but cloud properties are locked to those in different years from CTL-FOM	10	1-10	5
hNA-FOM-CL	As hNA-FOM but cloud properties are locked to those in different years from CTL-FOM	10	1-10	5